JOURNAL OF GEOPHYSICAL RESEARCH: ATMOSPHERES, VOL. 118, 1–11, doi:10.1002/jgrd.50216, 2013

Impact of model errors in convective transport on CO source estimates inferred from MOPITT CO retrievals

Zhe Jiang,[1] Dylan B. A. Jones,[1,2] Helen M. Worden,[3] Merritt N. Deeter,[3] Daven K. Henze,[4] John Worden,[5] Kevin W. Bowman,[2,5] C. A. M. Brenninkmeijer,[6] and T. J. Schuck[6]

Received 20 September 2012; revised 15 January 2013; accepted 22 January 2013.

[1] Estimates of surface fluxes of carbon monoxide (CO) inferred from remote sensing observations or free tropospheric trace gas measurements using global chemical transport models can have significant uncertainties because of discrepancies in the vertical transport in the models, which make it challenging to unequivocally relate the observations back to the surface fluxes in the models. The new Measurement of Pollution in the Troposphere (MOPITT) version 5 retrievals provide greater sensitivity to lower tropospheric CO over land relative to the previous versions and are, therefore, useful for evaluating vertical transport in models. We have assimilated the new MOPITT CO retrievals, using the Goddard Earth Observing System (GEOS)-Chem model, to study the influence of vertical transport errors on inferred CO sources. We compared the source estimates obtained by assimilating the CO profiles, the column amounts, and the surface level retrievals for June–August 2006. The three different inversions produced large differences in the source estimates in regions of convection and strong CO emissions. The inversion using the CO profiles suggested an 85% increase in emissions in India/Southeast Asia, which exacerbated the model bias in the lower and middle troposphere, whereas using the surface level retrievals produced a 37% decrease in Indian/Southeast Asian emissions, which exacerbated the underestimate of CO in the upper troposphere. Globally, the inversion with the surface retrievals suggested a 22% reduction in emissions from the a priori estimate of 161 Tg CO/month (from combustion and the oxidation of biogenic volatile organic compounds), averaged in June–August 2006. The analysis results were validated with independent surface CO measurements from NOAA Global Monitoring Division (GMD) network and upper troposphere CO measurements from the Civil Aircraft for the Regular Investigation of the Atmosphere Based on an Instrumented Container (CARIBIC). We found that the inversion with the surface retrievals agreed best with surface CO data but produced the largest discrepancy with the CARIBIC aircraft data in the upper troposphere, suggesting the influence of vertical transport errors in the model. Our results show that the comparison of the a posteriori CO distributions obtained from the inversions using the surface and profile retrievals provides a means of characterizing the potential impact of the vertical transport biases on the source estimates and the CO distribution.

Citation: Jiang, Z., D. B. A. Jones, H. M. Worden, M. N. Deeter, D. K. Henze, J. Worden, K. W. Bowman, C. A. M. Brenninkmeijer, and T. J. Schuck (2013), Impact of model errors in convective transport on CO source estimates inferred from MOPITT CO retrievals, *J. Geophys. Res. Atmos.*, *118*, doi:10.1029/jgrd.50216.

1. Introduction

[2] Atmospheric carbon monoxide (CO) is a product of incomplete combustion and a byproduct of the oxidation of hydrocarbons in the atmosphere. It plays a key role in controlling the oxidative capacity of the atmosphere since it is the main sink for the hydroxyl radical (OH), the primary tropospheric oxidant. Inverse modeling of atmospheric CO has been the focus of several studies during the past decade to better quantify regional emissions of CO. These inverse modeling studies have employed surface observations [e.g., *Pétron et al.*, 2002; *Kasibhatla et al.*, 2002; *Hooghiemstra et al.*, 2011], space-based measurements [e.g., *Pétron et al.*, 2004; *Heald et al.*, 2004; *Arellano et al.*, 2006, *Arellano and*

[1]Department of Physics, University of Toronto, Toronto, Ontario, Canada.
[2]JIFRESSE, University of California, Los Angeles, Los Angeles, California, USA.
[3]NCAR, Boulder, Colorado, USA.
[4]University of Colorado, Boulder, Colorado, USA.
[5]Jet Propulsion Laboratory, California Institute of Technology, Pasadena, California, USA.
[6]Max-Planck-Institut fur Chemie, Air Chemistry Division, Mainz, Germany.

Corresponding author: Z. Jiang, University of Toronto, Toronto, Ontario, M5S 1A7, Canada. (zjiang@atmosp.physics.utoronto.ca)

2169-897X/13/10.1002/jgrd.50216

Hess, 2006; *Kopacz et al*., 2010; *Jones et al*., 2009; *Fortems-Cheiney et al*., 2011; *Gonzi et al*., 2011; *Jiang et al*., 2011], and aircraft data [e.g. *Palmer et al*., 2003; *Heald et al*., 2004]. However, as discussed in *Jiang et al*. [2011], there is still significant uncertainty in estimates of the regional CO sources, reflecting, in part, the impact of systematic errors in the inversion analyses and the varying information content of the different datasets. In this context, systematic model errors in convective transport are a particular concern as *Tost et al*. [2010] have shown that the choice of convection scheme in a given model can result in discrepancies in the simulated distribution of CO as large as 20% globally and 100% locally.

[3] In their inversion analysis of CO profiles from the Measurement of Pollution in the Troposphere (MOPITT) instrument and the Tropospheric Emission Spectrometer (TES), *Jones et al*. [2009] found that their a posteriori CO emissions resulted in an overestimate of CO abundances relative to surface measurements in the southern hemisphere. *Arellano et al*. [2006] found that their a posteriori emission estimates, inferred from MOPITT column CO retrievals, overestimated the CO as observed from the surface sites in the southern hemisphere, which they speculated could be due to bias in transport in their model. These studies used the same version of the MOPITT data (version 3) and their results are suggestive of discrepancies in the vertical transport in the models employed in the inversion analyses. Recently, *Hooghiemstra et al*. [2011] found that the source estimates inferred from surface CO data improved the modeled CO relative to MOPITT data throughout the northern hemisphere, but underestimated the MOPITT data in the southern hemisphere. In their analysis, *Hooghiemstra et al*. [2011] used version 4 of the MOPITT data, but since the primary surface source of CO in the southern hemisphere is the biomass burning in regions such as South America, Africa, and Indonesia, where convective transport plays an important role in exporting the CO emissions to the free troposphere, the *Hooghiemstra et al*. [2011] results could also be due to the influence of transport biases. Ideally, in the absence of transport bias, the surface and satellite data should provide consistent constraints on the sources, if the data coverage is representative of the spatiotemporal variability in CO.

[4] With an observing strategy that achieves complete global coverage every 3 days, MOPITT provides dense sampling of the CO distribution. The newly available multispectral retrievals (version 5) exploit both the near-infrared (NIR) and the thermal infrared (TIR) spectral domains to obtain greater sensitivity to CO in the lower troposphere over land [*Deeter et al*., 2011] than previous remote sensing products, which were primarily sensitive to middle and upper tropospheric abundances or column amounts. The sensitivity to lower and upper tropospheric CO in the new MOPITT v5 retrievals offers a unique opportunity to assess here, using the Goddard Earth Observing System (GEOS)-Chem model, the impact of the surface level retrievals, the profiles, and the column amounts on the inferred CO source estimates in the context of potential biases in the vertical transport of CO in the model. We focus here on the June–August 2006 period, as a test case, when convective transport associated with the Asian monsoon has a significant impact on the atmospheric circulation and the distribution of CO in the troposphere.

2. Observations and Model

2.1. MOPITT

[5] The MOPITT instrument was launched on 18 December 1999, on NASA's Terra spacecraft in a sun-synchronous polar orbit at an altitude of 705 km, with a 10:30 local time equator crossing, and a spatial resolution of 22 × 22 km. In the version 5 retrievals, the TIR (4.7 μm) radiances are combined with the NIR (2.3 μm) radiances to significantly improve the sensitivity to lower tropospheric CO over land. The retrieved volume mixing ratios (VMR) are reported on 10 pressure levels (surface, 900, 800, 700, 600, 500, 400, 300, 200, and 100 hPa). Similar to the MOPITT version 4 data product [*Deeter et al*., 2010], the v5 retrievals are performed with respect to the logarithm of the CO VMR using an optimal estimation approach. The retrieved CO profiles can be expressed as a linear estimate of the true atmospheric state:

$$\hat{\mathbf{z}} = \mathbf{z}_a + \mathbf{A}(\mathbf{z} - \mathbf{z}_a) + \mathbf{G}\varepsilon \tag{1}$$

where $\mathbf{z}_a$ is the MOPITT a priori CO profile (expressed as log (VMR)), $\mathbf{z}$ is the true atmospheric state (also as log(VMR)), $\mathbf{G}\varepsilon$ describes the retrieval error, and $\mathbf{A} = \partial\hat{\mathbf{z}}/\partial\mathbf{z}$ is the MOPITT averaging kernel matrix, which gives the sensitivity of the retrieval to the actual CO in the atmosphere. Similar to the version 4 product, the version 5 retrievals use a monthly mean profile from the MOZART-4 CTM as the a priori information $\mathbf{z}_a$, which is significantly better than the fixed global profile used in the version 3 retrievals. In our analysis we construct CO column amount by integrating the retrieved CO profile, $\hat{c} = \mathbf{t}^T\hat{\mathbf{z}}$, where $\mathbf{t}$ is the column operator that includes both the conversion from VMR to number density and the vertical integration in the pressure coordinate.

[6] The main advantage of the MOPITT v5 TIR/NIR product over previous TIR-only retrievals is the use of the NIR spectral information over land to obtain greater sensitivity to CO in the lowermost troposphere over land. The zonal average degrees of freedom for signal (DFS) for the TIR-only retrievals is typically about 1.5 [*Deeter et al*., 2004], but *Worden et al*. [2010] have shown that the DFS for the TIR + NIR data are, on average, 32% greater over land. The MOPITT v5 retrievals can, therefore, provide independent constraints on lower and upper tropospheric CO. This can be seen in the averaging kernel rows shown in Figure 1. Over North America the surface sensitivity for summertime observations peaks strongly near 900 hPa, and the retrievals at 900, 800, and 700 hPa have peak sensitivities between 800 and 700 hPa, which decrease rapidly into the upper troposphere. In the upper troposphere, the retrievals at 400, 300, and 200 hPa have peak sensitivity at about 300 hPa, which decreases significantly with depth into the lower troposphere. The comparison of the averaging kernel over North America to that over Southeast Asia or across the tropics (between 10°S and 10°N) shows that there is less lower tropospheric sensitivity in these regions due to the fact that the Southeast Asian region and the tropical band between 10°S and 10°N include a large number of observations over the ocean, where the retrievals are actually based only on TIR measurements.

[7] The MOPITT v5 data are new and have not been as well validated as the previous versions of the retrievals. Therefore, we have conducted an indirect validation of the

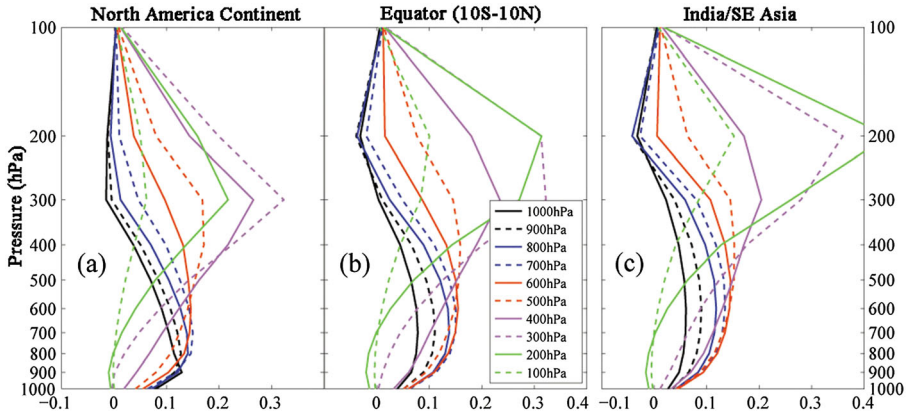

Figure 1. Regional mean MOPITT averaging kernel rows for June–August 2006. The boundaries for these regions are shown in Figure 6b. The North American region contains only land observations, whereas the equatorial and Indian/Southeast Asian regions include many ocean scenes. The weak lower tropospheric sensitivity in curve b and curve c is caused by the large number of ocean scenes, where the retrievals are based only on TIR measurements.

data by assimilating the MOPITT v4 and v5 retrievals separately into the GEOS-Chem model, using a sequential suboptimal Kalman filter [*Parrington et al.*, 2008]. The data were assimilated from 1 April 2006 to 31 August 2006, and the zonal mean relative differences between the v4 and v5 assimilated CO fields for June–August are shown in Figure 2. In general, the two assimilated data sets agree well from the surface to about 300 hPa. In the extratropics, the v5 assimilated CO fields are about 5% smaller in the lower and middle troposphere and about 10% larger between 300 and 200 hPa. At higher altitudes, above 200 hPa, the v5 assimilated fields are significantly greater, which could be due to biases in the MOPITT v5 retrievals at 150 hPa. As described below, in our inversion analyses, we use only MOPITT v5 retrievals at altitudes below 200 hPa.

2.2. GEOS-Chem

[8] The GEOS-Chem global chemical transport model (CTM) (data are available at http://www.geos-chem.org) is driven by assimilated meteorological observation from the NASA GEOS-5 at the Global Modeling and Data Assimilation Office. We use version v8-02-01 of GEOS-Chem, at a horizontal resolution of $4° \times 5°$. Our analysis is based on the CO-only simulation in GEOS-Chem, which uses archived monthly OH fields from the full chemistry run. The global anthropogenic emission inventory is EDGAR 3.2FT2000 [*Olivier and Berdowski*, 2001] but is updated by the following regional emission inventories: the US Environmental Protection Agency National Emission Inventory for 1999 [*Hudman et al.*, 2008] in North America, the Criteria Air Contaminants inventory for Canada, the Big Bend Regional Aerosol and Visibility Observational (BRAVO) Study Emissions Inventory for Mexico [*Kuhns et al.* 2003], the Cooperative Program for Monitoring and Evaluation of the Long-range Transmission of Air Pollutants in Europe (EMEP) inventory for Europe in 2000 [*Vestreng and Klein*, 2002], and the Streets and Zhang Asia emissions inventory for 2006 [*Zhang et al.*, 2009]. Biomass burning emissions are from the interannual GFED2 inventory with monthly resolution [*van der Werf et al.*, 2006]. Additional CO sources come from oxidation of methane and biogenic volatile organic compounds (VOCs,) as described in previous studies [e.g., *Kopacz et al.*, 2010; *Jiang et al.* 2011]. The global anthropogenic source (60°S–60°N) of CO from fossil fuel and biofuel combustion is 50.2 Tg/month. The global source of CO from biomass burning and non-methane volatile organic compounds (NMVOCs) is 41.0 Tg/month and 69.9 Tg/month, respectively. Figure 3 shows the monthly mean CO emission distribution for June–August 2006.

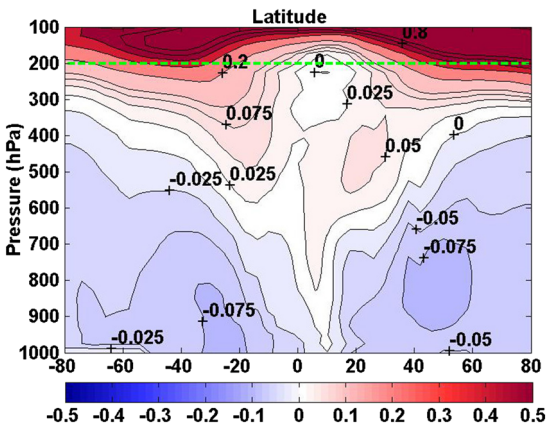

Figure 2. Zonal mean relative bias in assimilated CO fields with MOPITT v4 and v5, calculated as $(v5 - v4)/v4$, for June–August 2006. The v5 data at and above 200 hPa (green dashed line) are not used in this work.

[9] When comparing the GEOS-Chem model simulation with MOPITT observations, the modeled CO has to be smoothed with the MOPITT averaging kernels. Using the linear expansion of the retrieval, equation (1), the model is transformed as follows:

$$\hat{\mathbf{z}}^m = \mathbf{z}_a + \mathbf{A}(\mathbf{z}^m - \mathbf{z}_a) \tag{2}$$

where $\mathbf{z}^m$ is the raw modeled profile. Equation (2) is the observation operator, which is used to calculate the cost function and the maps, presented in Section 4, of the relative biases between the model and the MOPITT data.

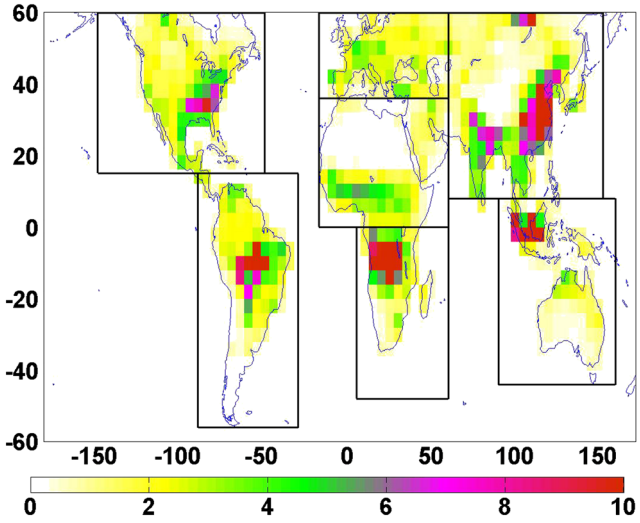

Figure 3. Monthly mean CO emissions from combustion sources and the oxidation of biogenic NMVOC, averaged for June–August 2006. The unit is 10^8 kg/month. The black boxes define the regions used for the budget analysis in Table 1.

3. Inversion Approach

[10] The inverse method seeks an optimal estimate of the CO sources that is consistent with both the observed atmospheric concentrations and the a priori constraints on the sources by minimizing the cost function $J(\mathbf{x})$,

$$J(\mathbf{x}) = (\mathbf{F}(\mathbf{x}) - \mathbf{y})^{\mathbf{T}}\mathbf{S}_{\Sigma}^{-1}(\mathbf{F}(\mathbf{x}) - \mathbf{y}) + (\mathbf{x} - \mathbf{x}_a)^{\mathbf{T}}\mathbf{S}_a^{-1}(\mathbf{x} - \mathbf{x}_a) \quad (3)$$

where $\mathbf{x}$ is the state vector of emissions, $\mathbf{y}$ is the observed concentrations, and $\mathbf{F}(\mathbf{x})$ is the forward model, as described in *Jones et al*. [2009], which represents the transport of the CO emissions in the GEOS-Chem model and accounts for the vertical smoothing of the MOPITT retrieval, described in equation (2). Here $\mathbf{x}_a$ is the a priori estimate and $\mathbf{S}_{\Sigma}$ and $\mathbf{S}_a$ are the observational and a priori error covariance matrices, respectively. The first term on the right in equation (3) represents the mismatch between the simulated and observed concentrations weighted by the error covariance of the system. The second term represents the departure of the estimate from the a priori. The cost function in equation (3) is minimized using the adjoint of GEOS-Chem model in a four-dimensional variational (4D-var) approach [*Henze et al*., 2007], which has been previously used for assimilation of CO and ozone [e.g., *Kopacz et al*., 2010; *Singh et al*. 2011; *Jiang et al*., 2011; *Parrington et al*., 2012].

[11] A fundamental assumption in minimizing equation (3) is that the observation and model errors are Gaussian. We focus here on the impact of vertical transport biases in the model on the source estimates. Biases in the data will also adversely impact the inferred source estimates. To avoid the influence of the positive observation bias in 200–100 hPa layer shown in Figure 2 and to minimize the effects of the stratosphere on the inversion, we neglected the highest two MOPITT levels (200 and 100 hPa) in the analyses. But in transforming the modeled profile into the MOPITT observation space using the averaging kernels and a priori profiles, we employ the full model profile from the surface to the top of the atmosphere. We also reject MOPITT data with CO column amounts less than 5×10^{17} mol/cm^2 and with low-cloud observations. Since the NIR radiances measure reflected solar radiation, only daytime data are considered here. We assimilate MOPITT data from June–August 2006 and conduct three different inversion analyses to examine the impact of the vertical information from the MOPITT retrievals on the source estimates. We compare assimilations based on (1) the tropospheric profiles at altitudes below 200 hPa (the 300 hPa MOPITT retrieval layer), (2) the tropospheric column amounts (integrated up to 200 hPa), and (3) the surface level retrievals only.

[12] As in the work of *Jiang et al*. [2011], we assume a uniform observation error of 20% to account for representativeness errors and the influence of random transport errors in the model. This will overestimate the errors for ocean scenes, but it will underestimate it for lower tropospheric retrievals over land. However, as shown by *Heald et al*. [2004], the estimates from the main source regions are relatively insensitive to the observation errors since these errors are assumed to be random and because we are assimilating a large number of observations (about 66,000 in the case of the surface level inversion). Because the CO observations provide constraints only on the total CO emitted from a given region, there is insufficient information in the inversion to reliably distinguish different CO source types. Following *Jiang et al*. [2011], we combine the combustion CO sources (fossil fuel, biofuel, and biomass burning) with the CO from the oxidation of biogenic NMVOCs and solve for the total CO emissions in each grid box, assuming a 50% uniform a priori error. The source of CO from the oxidation of methane is aggregated into a global source, which we optimize assuming an a priori uncertainty of 25%. We also assume that the a priori error covariance matrix $\mathbf{S}_a$ is diagonal.

[13] Because the lifetime of CO is about 2 months, model errors can accumulate and bias the initial CO distribution at the beginning of the assimilation period, which, in turn, would bias the top-down source estimates. We produce an improved initial condition by assimilating MOPITT v5 data, using the sequential suboptimal Kalman filter, between 1 April 2006 and 31 May 2006. This provides a distribution of CO on 1 June 2006 (the beginning of the assimilation period) that is in better agreement with the MOPITT data than the free running model. Figure 4a shows the model bias in 25–31 May 2006, with the original GEOS-Chem initial conditions. The model significantly underestimates the CO abundances across the northern extratropics. The zonal mean bias in the CO columns in the extratropics (20°N–60°N) decreased from −24.0% to 0.2% with the Kalman filter assimilation (Figure 4b). As a result of the optimized initial conditions at the end of May 2006, discrepancies between the model and MOPITT during June to August will either reflect errors in the prescribed CO sources in the model or biases in the model transport. The objective of the inversion analysis is to use the mismatch between the model and MOPITT to obtain an improved estimate of the CO sources for the June–August 2006 period.

4. Results and Discussion

[14] The scaling factors, which are the ratio of the a posteriori emission estimates to the a priori values, are shown

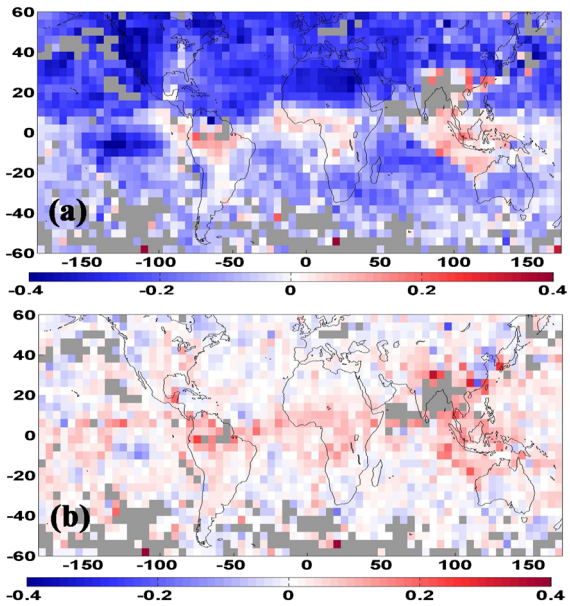

Figure 4. Relative model bias in column CO, calculated as (model − MOPITT) / MOPITT. (a) Bias in 25–31 May 2006, with the original GEOS-Chem initial condition. (b) Bias in 25–31 May 2006, with the Kalman filter assimilation. The grey grids correspond to MOPITT data gaps.

in Figure 5 for the inversion analyses based on the three MOPITT data sets described in Section 3: the retrieved CO profile, the column abundances, and the surface level retrievals. The first-order spatial patterns of the changes in the emissions (Figures 5a, 5b, and 5c) are similar for the inversions: CO emissions in low-latitude regions were reduced, whereas emissions in the midlatitudes were increased. The regional mean scaling factors, averaged for the regions shown in Figure 3, are listed in Table 1. The a posteriori emission estimates obtained with the surface level retrievals are the lowest in most regions. The differences between the regional estimates from the three inversions are typically about 15% or less. The most significant discrepancy between the three emission estimates is for the Asian region for which the inversion using the profiles suggests an 11% increase in a priori Asian emissions, whereas the surface level retrievals suggest a 30% decrease.

[15] The biases in the a priori and a posteriori modeled CO columns are shown in Figure 6. Since the initial conditions on 1 June 2006 were optimized to match the MOPITT data, the model bias during the assimilation period is most pronounced in the tropics, in the vicinity of the Intertropical Convergence Zone (ITCZ). The largest model biases are over Central America and over India/Southeast Asia, where the convective mass fluxes are largest in the middle troposphere (Figure 6b). All three inversions reduced this model bias; however, the inversion with the profile data enhanced the model bias over India/Southeast Asia, suggesting that the a posteriori emission estimates for this region are biased. Indeed, the profile inversion suggests an 85% increase in the Indian/Southeast Asian emissions (averaged over the strong convection region shown in Figure 6b), whereas the column and surface level inversions produced a reduction in emissions of 17% and 37%, respectively. Although there are residual positive biases in the CO columns in the convection regions in the tropics in all three inversions, we find that the surface level inversion provides the largest reduction of the a priori positive model bias. However, the negative column bias is magnified in some regions, which, as we describe

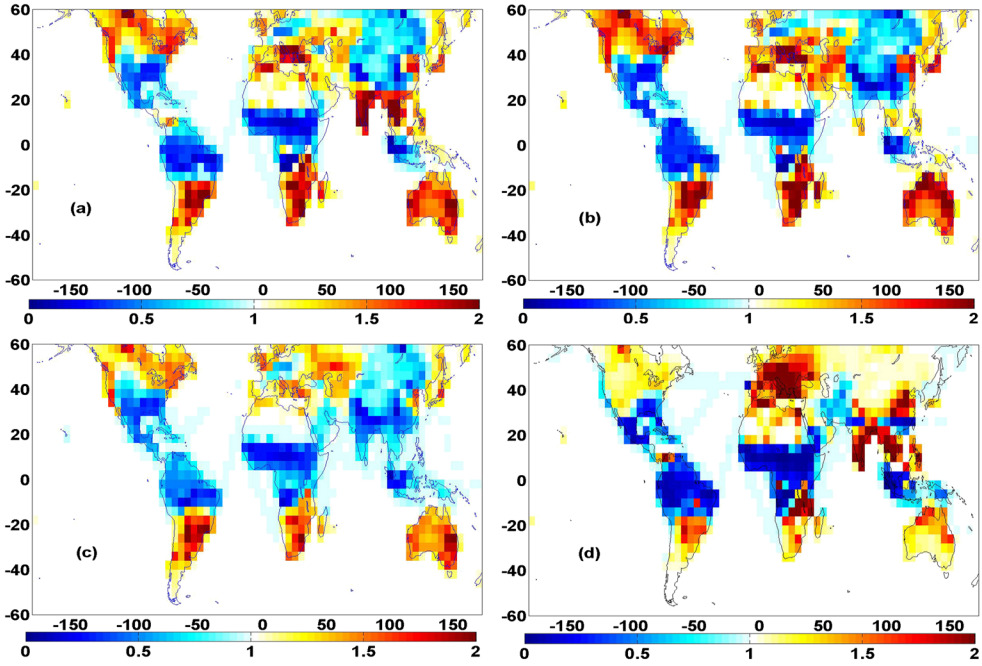

Figure 5. Scaling factors, which are the ratio of the a posteriori to the a priori emissions, for (a) the profile inversion, (b) the column inversion, (c) the surface level inversion, and (d) the profile inversion with MOPITT observations only in the tropics, between 10°S and 25°N. The color scale is saturated at 2, but the scaling factors is larger than 2 in some grid boxes.

Table 1. A Priori and a Posteriori CO Emission and Scaling Factors for June–August 2006

Inversion Type	Regions								
	Global	North America	Europe	Asia	South America	North Africa	South Africa	Indo/Australia	
A priori (Tg/month)	**161.0**	**23.0**	**15.0**	**43.8**	**23.8**	**15.7**	**22.5**	**16.9**	
Scaling factor	Profile inversion	**150.1**	**22.0**	**17.8**	**48.4**	**18.5**	**8.0**	**22.3**	**12.6**
		0.93	0.96	1.19	1.11	0.78	0.51	0.99	0.75
	Column inversion	**141.9**	**23.1**	**18.8**	**37.4**	**18.0**	**8.6**	**22.4**	**13.0**
		0.88	1.00	1.25	0.85	0.76	0.55	1.00	0.77
	Surface inversion	**125.3**	**20.1**	**18.0**	**30.8**	**18.4**	**7.6**	**18.3**	**11.7**
		0.78	0.87	1.20	0.70	0.77	0.48	0.81	0.69

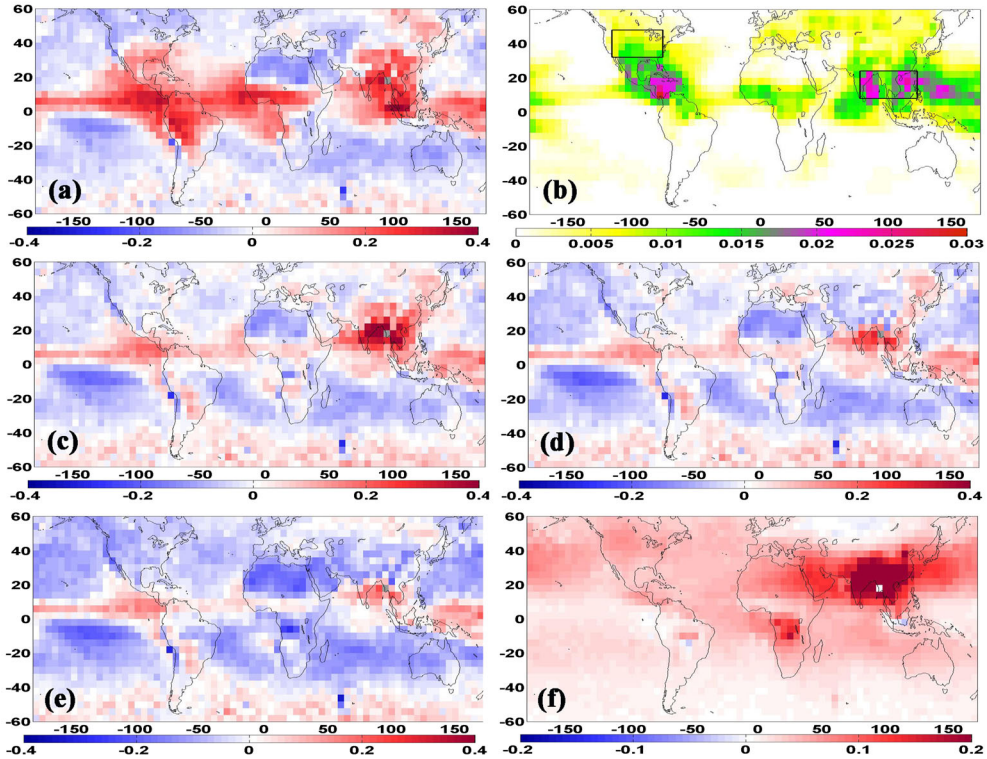

Figure 6. Relative model bias in column CO (surface to 200 hPa), calculated as (model − MOPITT)/MOPITT, for June–August 2006 for CO estimated with (a) the a priori emissions and the a posteriori emissions from (c) the profile inversion, (d) the column inversion, and (e) the surface level inversion. (f) Impact on CO distribution shows the difference between the results in Figures 6c and 6e. Figure 6b shows the mean convective mass flux (400 hPa − 500 hPa) in units of kg/m2/s in June–August 2006. The black boxes in Figure 6b define the regions for Figures 1 and 7.

below, is because the surface inversion exacerbates the model bias in the upper troposphere.

[16] The vertical structure of the mean model bias aggregated for North America, the tropics, and India/Southeast Asia is shown in Figure 7. In all three regions the model is biased high in the middle and lower troposphere and biased low in the upper troposphere relative to MOPITT. Over North America the model bias is less than about 10% throughout the lower and middle troposphere and increases to −13% at the 300 hPa MOPITT level (300–200 hPa layer). The model bias is larger across the tropics, particularly over the Indian/Southeast Asian region, where it is about 35–40% in the middle troposphere and −10% at the 300 hPa MOPITT level. *Gonzalez Abad et al.* [2011] also found that the model overestimated CO in the middle troposphere and underestimated it in the upper troposphere in the tropics in their comparison of GEOS-Chem with CO measured by the Atmospheric Chemistry Experiment Fourier Transform Spectrometer (ACE-FTS). The assumption in the CO-only mode of GEOS-Chem that the VOC source of CO can be represented as a surface source, reflecting instantaneous oxidation of the VOCs, could also contribute to the overestimate of CO in the lower troposphere and the underestimate in the upper troposphere. Sensitivity runs using the tagged CO simulation in GEOS-Chem suggest that the VOC source contributes about 30% of the CO in the upper troposphere over Southeast Asia; therefore, attributing the cause of the observed bias in CO to the VOC source in the model would require significantly large uncertainties in the surface VOC emissions. GEOS-5 employs the Relaxed Arakawa Shubert

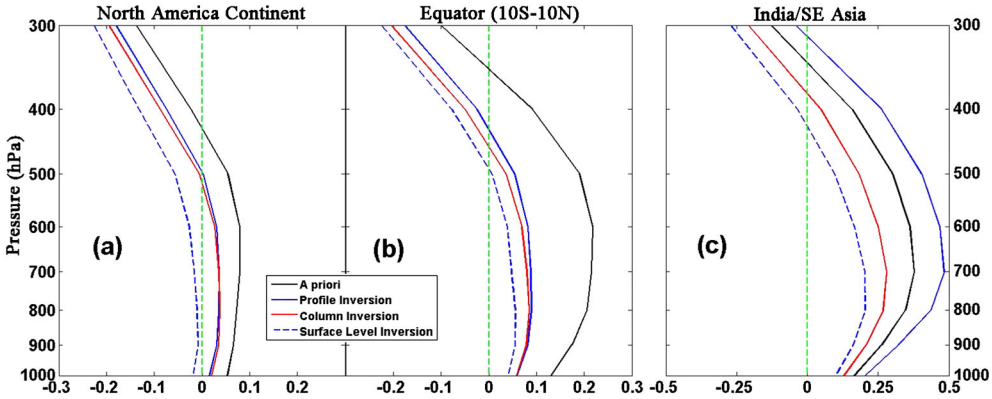

Figure 7. Vertical profile of the relative regional model bias, calculated as (model − MOPITT) / MOPITT, for June–August 2006. The modeled profiles were transformed with the MOPITT averaging kernels and a priori profiles. The boundaries for these regions are shown in Figure 6b. The *x* axis is different in each curve to better illustrate the changes in the model bias in each region with the three inversions.

(RAS) convection scheme [*Arakawa and Schubert*, 1973], and *Folkins et al*. [2006] and *Ott et al*. [2009] have shown that the RAS scheme underestimates the convective mass fluxes and places the convective outflow too low in altitude, which would account for the model biases shown in convection region Figure 7c. Recent studies [*Huang et al*., 2012; *Liu et al*., 2012], showed that observations of CO from the Microwave Limb Sounder (MLS) indicate strong vertical transport of CO in the upper troposphere over the Asian monsoon region, between 10°N and 30°N. *Liu et al*. [2012] found that the vertical transport in GEOS-Chem, with GEOS-5 meteorological fields, is too weak in this region.

[17] Across the tropics and over North America, the profile and column inversions produce similar residual biases between MOPITT and the a posteriori CO simulations. In these regions the inversions reduced the model bias in the middle and lower troposphere, but exacerbated the negative model bias in the upper troposphere. Over India/Southeast Asia, on the other hand, the profile inversion enhanced the positive model bias in the lower and middle troposphere, but reduced the model bias in the upper troposphere. Large discrepancies between the three inversions are observed in regions where strong convection coincides with high emissions of CO. India/Southeast Asia and Central America are the major deep convection regions in June–August 2006. However, emissions are significantly greater in Southeast Asia than in Central America (see Figure 3). As a result, the profile inversion increases Indian/Southeast Asian emissions to reduce the negative model bias in the upper troposphere. Indeed, observations of CO by MLS show the maximum in CO concentrations over Southeast Asia at 200 hPa [*Filipiak et al*., 2005; *Li et al*., 2005; *Park et al*., 2007, 2009], where the MOPITT averaging kernels are strongly peaked (shown in Figure 1c). Using the column data mitigates the impact of the model bias in the upper troposphere and, thus, the column inversion produces a reduction in the CO emissions in this region. As expected, using the surface level retrievals produced an even greater reduction in the emissions in this region since these retrievals are sensitive mainly to CO in the lower and middle troposphere, where the model is highly biased. To assess the impact of possible biases in the MOPITT data as reflected in the larger extratropical differences between the v4 and v5 assimilated fields shown in Figure 2, we conducted an additional inversion analysis using MOPITT profiles only between 10°S and 25°N, where the v4 and v5 assimilated fields were consistent. In the tropics, the inversion results (Figure 5d) are similar to those obtained using full MOPITT coverage (Figure 5a). Thus, we believe that the enhanced a posteriori model bias obtained in the Indian/Southeast Asian region with the profile inversion is not due to the possible biases in the MOPITT retrievals.

[18] The difference between the profile and surface level inversion reflects the impact of the transport bias on the CO field. As shown in Figure 6f, the impact on the CO distribution is mainly within the Tibetan anticyclone region (over South Asia and the Middle East) but extends across the North Pacific to North America. There is also a large impact over the source region in central Africa. The CO feature over Asia and across the north Pacific is typical of the CO outflow pattern from the summertime Asian monsoon, which *Jiang et al*. [2007] showed is linked to the summertime maximum in upper tropospheric CO abundances over the Pacific.

[19] To better understand the nature of the model bias shown in Figure 7, we assimilated the MOPTT data to optimize the CO initial distribution (a state optimization) through the month of June 2006. We assimilated the data in 10-day intervals, on 1–10, 11–20, and 21–30 June 2006, using the a posteriori CO emissions of the surface level inversion. The motivation is that in optimizing the emissions (a source optimization), the model is employed as a transfer function that relates the emissions to the observations, therefore, if the model transport is biased there will be residual biases between the observation and the modeled CO obtained with the a posteriori emissions. On the other hand, optimizing the CO initial distribution forces the modeled CO to match the observations as best as possible over the assimilation period, given the uncertainty of the model and observations. As expected, the residual model bias in the upper troposphere in the state optimization, shown in Figures 8b, 8d, and 8f, is small in each 10-day interval. In contrast, as shown in Figure 8a, when we ran the model over the 1–10 June 2006 period without assimilation; starting from the same initial conditions that were used in the state optimization in Figure 8b, we obtained larger residual model biases in the upper

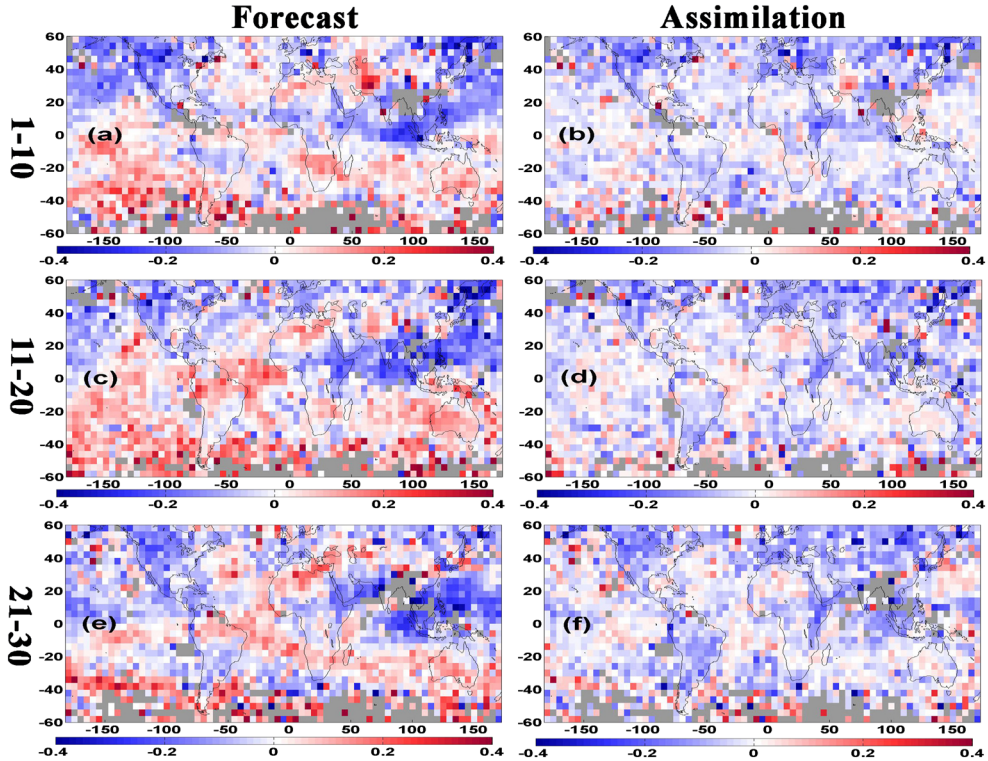

Figure 8. Relative residual bias at 300 hPa in June 2006, calculated as (model – MOPITT) / MOPITT. Figures in row 1 (Figures 8a and 8b), row 2 (Figures 8c and 8d), and row 3 (Figures 8e and 8f) show the results from the assimilation experiments for 1–10, 11–20, and 21–30 June 2006, respectively. The (a, c, and e) forecast plots show the residual bias in the forward model simulation of CO, whereas the (b, d, and f) assimilation plots show the residual bias from the state optimization for the initial CO distribution. For each 10-day period, the forecast and assimilation runs were initiated with same initial conditions. For the simulations starting on 1 June 2006 (Figures 8a and 8b), the initial conditions were obtained from assimilation of data in May 2006. The initial conditions for the runs on 11 and 21 June 2006 were obtained from the optimized state from the previous 10 days, in Figures 8b and 8d, respectively.

troposphere. Despite the fact that the model was forced with the a posteriori emissions, the model bias shown in Figure 8a emerged over the 10-day period, with the largest bias over the Asian monsoon region. Similarly large residual model biases emerged during the 11–20 and 21–30 June 2006 intervals when we ran the model without optimizing the state (Figures 8c and 8e). Given the long lifetime of CO, discrepancies in transport are likely to be the main source of the rapid growth of this model bias in the upper troposphere.

[20] The large negative model bias in upper troposphere in the Asian monsoon region, as shown in Figures 8a, 8c, and 8e, is the major driven force for the increase of CO emission in India/Southeast Asia in the profile inversion. As explained above, it is in this region that CO is at a maximum in the upper troposphere, so the inversion strongly adjusts the Asian emissions to compensate for the model bias. On the other hand, the negative model bias in the Asian monsoon region is not present in the inversion with the column data since the model bias in the tropospheric column is dominated by the positive bias in the lower and middle troposphere (Figure 6a). The overestimate in the model column leads to the emission reduction shown in Figure 5b.

[21] We note that a potential factor influencing the inversion in the tropics could be the lower data density due to cloud cover in regions of convection. The inversion could over-adjust the emissions in regions with low data density since these regions will contribute less to the cost function. We examined this by conducting a profile inversion in which we weighted the first term in the cost function, equation (3), to ensure that each grid box with observations contributed equally to the cost function. We found that this did not significantly change the residual model bias shown in Figure 6, suggesting that the non-uniform observational coverage has a limited impact on our results.

[22] We compared the a priori and a posteriori model simulations with data from the NOAA Global Monitoring Division (GMD) network (GMD data were obtained from ftp://ftp.cmdl.noaa.gov/ccg/co/flask/event/). We selected the data between June and August 2006 from 48 stations across the globe, as shown in Figure 9. Since each station only has a small number of observations during the three-month period, we focus on global statistics to assess the fidelity of the modeled simulation. In Figure 10, all three inversions improved the CO distribution relative to surface in situ observation. As expected, the CO distribution from the inversion using the surface level retrievals best agrees with the GMD data, with a mean model bias of 2.7 ppb compared to the a priori model bias of 7.8 ppb.

[23] To evaluate the model simulation in the upper troposphere we compare the modeled CO to data from the Civil

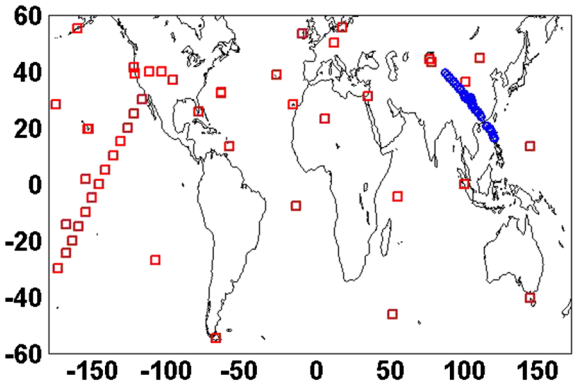

Figure 9. Global distribution of CO flask sample collection locations from 48 NOAA GMD sites (red squares) and aircraft sampling locations from CARIBIC (blue circles).

Aircraft for the Regular Investigation of the Atmosphere Based on an Instrumented Container (CARIBIC) aircraft measurements [*Brenninkmeijer et al.*, 2007; *Scharffe et al.*, 2012]. There were two round-trip flights along the Frankfurt (Germany) to Guangzhou (China) to Manila (Philippines) route during June–August 2006 (5–7 July and 31 July to 2 August 2006), with cruising altitude at about 11 km (Figure 9). To restrict the comparison to locations in the troposphere we only used the observation data south of 40°N. As shown in Figure 11, the profile inversion improved the model simulation relative to CARIBIC data, reducing the model bias from −2.9 ppb to 0.1 ppb. On the other hand, both the column inversion and surface level inversions significantly magnified the negative model bias in upper troposphere. The opposite impact of surface level inversion on the model agreement with the independent data at the surface and in the upper troposphere suggests the presence of vertical transport errors in the inversion.

5. Summary

[24] We have examined the potential impact of vertical transport model errors on inferred CO source estimates using the new version 5 MOPITT retrievals. We have shown that inverse modeling of CO emissions using the surface level MOPITT retrievals, the tropospheric profiles, or the CO column amounts can produce significant differences in the inferred source estimates in regions of convection and strong CO emissions in the model. The inversion using the CO profiles suggested an 85% increase in emissions in India/Southeast Asia, which exacerbated the model bias in the lower and middle troposphere, whereas using the surface level retrievals produced a 37% decrease in Indian/Southeast Asian emissions, which exacerbated the underestimate of CO in the upper troposphere. In general, the a posteriori CO distribution obtained from the inversion using the surface level MOPITT retrievals produced the smallest residual model bias relative to MOPITT in the lower and middle

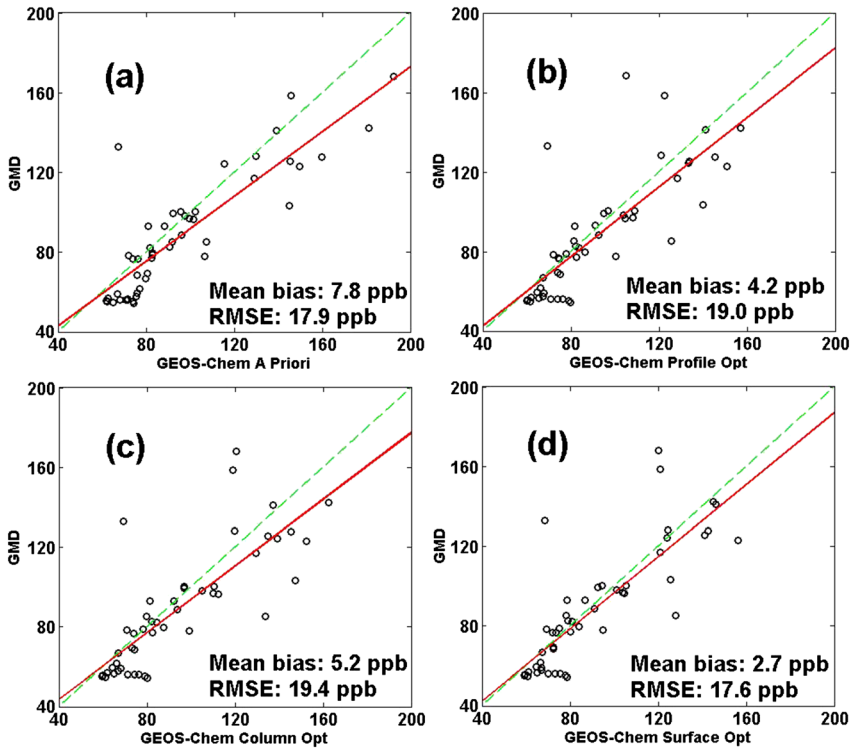

Figure 10. Scatter plots comparing model simulation with NOAA GMD surface observation, in June−August 2006, for (a) the a priori simulation, (b) the a posteriori simulations of the profile inversion, (c) the a posteriori simulations of the column inversion, and (d) the a posteriori simulations of the surface level inversion. Measured GMD CO abundance in ppb mole fraction was referenced to the NOAA/WMO 2004 scale. The modeled CO is sampled at the GMD observation time and location in ppb. The mean model bias (model minus observation) and the root-mean-square error (RMSE) are calculated for each case. The red line shows the linear fit, whereas the green dashed line shows the 1:1 relationship.

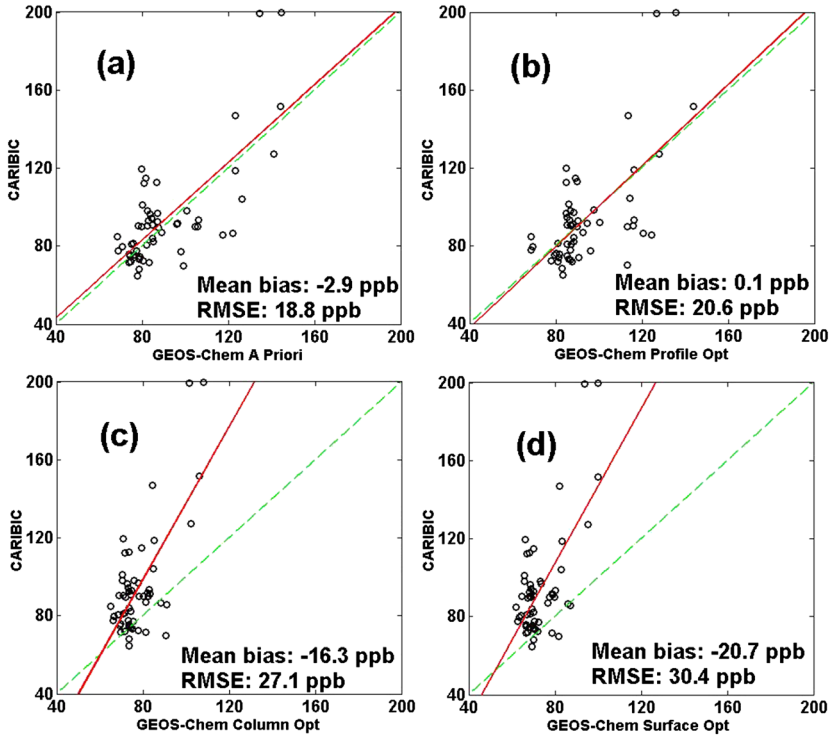

Figure 11. Scatter plots comparing model simulation with CARIBIC aircraft observation, in June−August 2006, for (a) the a priori simulation, (b) the a posteriori simulations of the profile inversion, (c) the a posteriori simulations of the column inversion, and (d) the a posteriori simulations of the surface level inversion. Only CARIBIC observations south of 40°N are used. The modeled CO is sampled at the aircraft observation time and location in ppb. The mean model bias (model minus observation) and the root-mean-square error (RMSE) are calculated for each case. The red line shows the linear fit, whereas the green dashed line shows the 1:1 relationship.

troposphere and agreed best with independent surface CO data. However, the surface level inversion exacerbated the model bias in the upper troposphere relative to independent aircraft data from CARIBIC. Similar results were obtained by *Nassar et al.* [2011] in their inversion analysis of CO_2 data from TES and the GMD network, also using GEOS-Chem. Their inversion analysis of the GMD surface CO_2 data produced a posteriori CO_2 fields that were in better agreement with independent surface data, but which exacerbated the model disagreement with aircraft data in the upper troposphere, suggesting the influence of vertical transport errors in the model.

[25] Accounting for the influence of vertical transport biases on the inversion analyses of long-lived gases such as CO, CO_2, and CH_4 is clearly important. However, characterizing vertical transport biases is challenging. The new multi-spectral v5 MOPITT data provide a valuable dataset for evaluating vertical transport and characterizing the biases in models. Because of the greater sensitivity to lower tropospheric CO in the v5 retrievals, compared to the previous versions of the retrievals, the use of the lower tropospheric v5 data in an inversion produces source estimates that depend mainly on the lower tropospheric loading of CO. In contrast, inversions using upper tropospheric CO retrievals rely on the vertical transport in the model to relate the CO surface emissions to the observed CO. Our results show that comparison of the a posteriori CO distributions obtained from inversions using the surface and profile retrievals provides a means of characterizing the potential impact of the vertical transport biases on the source estimates and the CO distribution.

[26] **Acknowledgments.** This work was supported by funding from the Natural Science and Engineering Research Council of Canada, the Canadian Space Agency, and NASA grants NNX10AT42G and NNX09AN77G. We thank NOAA ESRL for providing their CO flask data. We also acknowledge useful discussions with Susan Kulawik.

References

Arakawa, A., W. H. Schubert (1973), Interaction of a cumulus cloud ensemble with the large-scale environment: Part I, *J. Atmosp. Sci.*, *31*, 674.

Arellano, A. F., Jr., and P. G. Hess, (2006), Sensitivity of top-down estimates of CO sources to GCTM transport, *Geophys. Res. Lett.*, *33*, L21807.

Arellano, A. F., Jr., et al. (2006), Time dependent inversion estimates of global biomass-burning CO emissions using measurement of pollution in the troposphere (MOPITT) measurements, *J. Geophys. Res.*, *111*, D09303.

Brenninkmeijer, C. A. M., et al. (2007), Civil aircraft for the regular investigation of the atmosphere based on an instrumented container: The new CARIBIC system, *Atmos. Chem. Phys.*, *7*, 4953–4976.

Deeter, M. N., et al. (2004), Vertical resolution and information content of CO profiles retrieved by MOPITT, *Geophys. Res. Lett.*, *31*, L15112.

Deeter, M. N., et al. 2010, The MOPITT version 4 CO product: Algorithm enhancements, validation, and longterm stability, *J. Geophys. Res.*, *115*, D07306.

Deeter, M. N., et al. (2011), MOPITT multispectral CO retrievals: Origins and effects of geophysical radiance errors, *J. Geophys. Res.*, *116*, D15303.

Filipiak, M. J., et al. (2005), Carbon monoxide measured by the EOS Microwave Limb Sounder on Aura: First results, *Geophys. Res. Lett. 32*, L14825.

Folkins, I., et al. (2006), Testing convective parameterizations with tropical measurements of HNO3, CO, H2O, and O3: Implications for the water vapor budget, *J. Geophys. Res.*, *111*, D23304.

Fortems-Cheiney, A., et al. (2011), Ten years of CO emissions as seen from measurements of pollution in the troposphere (MOPITT), *J. Geophys. Res.*, *116*, D05304.

Gonzalez Abad, G., et al. (2011), Ethane, ethyne and carbon monoxide concentrations in the upper troposphere and lower stratosphere from ACE and GEOS-Chem: A comparison study, *Atmos. Chem. Phys.*, *11*, 9927–9941.

Gonzi, S., L. Feng, and P. I. Palmer (2011), Seasonal cycle of emissions of CO inferred from MOPITT profiles of CO: Sensitivity to pyroconvection and profile retrieval assumptions, *Geophys. Res. Lett.*, *38*, L08813, doi:10.1029/2011GL046789.

Heald, C. L., et al. (2004), Comparative inverse analysis of satellite (MOPITT) and aircraft (TRACE-P) observations to estimate Asian sources of carbon monoxide, *J. Geophys. Res. 109*, D23306.

Henze, D. K., A. Hakami and J. H. Seinfeld (2007), Development of the adjoint of GEOS-Chem, *Atmos. Chem. Phys.*, *7*, 2413–2433.

Hooghiemstra, P. B., et al. (2011), Optimizing global CO emission estimates using a four-dimensional variational data assimilation system and surface network observations, *Atmos. Chem. Phys.*, *11*, 4705–4723.

Huang, L., R. Fu, J. H. Jiang, J. S. Wright, and M. Luo (2012), Geographic and seasonal distributions of CO transport pathways and their roles in determining CO centers in the upper troposphere, *Atmos. Chem. Phys. 12*, 4683–4698.

Hudman, R. C., et al. (2008), Biogenic versus anthropogenic sources of CO in the United States, *Geophys. Res. Lett.*, *35*, L04801.

Jiang, J. H., et al. (2007), Connecting surface emissions, convective uplifting, and long-range transport of carbon monoxide in the upper troposphere: New observations from the Aura Microwave Limb Sounder, *Geophys. Res. Lett.*, *34*, L18812.

Jiang, Z., et al. (2011), Quantifying the impact of model errors on top-down estimates of carbon monoxide emissions using satellite observations, *J. Geophys. Res.*, *116*, D15306.

Jones, D. B. A., et al. (2009), The zonal structure of tropical O3 and CO as observed by the Tropospheric Emission Spectrometer in November 2004. Part I: Inverse modeling of CO emissions, *Atoms. Chem. Phys.*, *9*, 3547–3562.

Kasibhatla, P., et al. (2002), Top-down estimate of a large source of atmospheric carbon monoxide associated with fuel combustion in Asia, *Geophys. Res. Lett.*, *29*(19), 1900.

Kopacz, M., et al. (2010), Global estimates of CO sources with high resolution by adjoint inversion of multiple satellite datasets (MOPITT, AIRS, SCIAMACHY, TES), *Atoms. Chem. Phys.*, *10*, 855–876.

Kuhns, H., M. Green, and V. Etyemezian (2003), Big Bend Regional Aerosol and Visibility Observational (BRAVO) Study Emissions Inventory, *Report prepared for BRAVO Steering Committee*, Desert Research Institute, Las Vegas, Nevada.

Li, Q. B., et al. (2005), Convective outflow of South Asian pollution: A global CTM simulation compared with EOS MLS observations, *Geophys. Res. Lett. 32*, L14826.

Liu, J., J. A. Logan, L. T. Murray, H. C. Pumphrey, M. J. Schwartz, and I. A. Megretskaia (2012), Transport analysis and source attribution of seasonal and interannual variability of CO in the tropical upper troposphere and lower stratosphere, *Atmos. Chem. Phys. Disc. 12*, 17397–17442.

Nassar, R. D. B. A., et al. (2011), Inverse modeling of CO2 sources and sinks using satellite observations of CO2 from TES and surface flask measurements, *Atoms. Chem. Phys.*, *11*, 6029–6047.

Olivier, J. G. J., and J. J. M. Berdowski (2001), Global emissions sources and sinks, in *The Climate System*, Swits & Zeitlinger, Lisse

Ott, L. E., et al. (2009), Analysis of convective transport and parameter sensitivity in a single column version of the Goddard Earth Observation System, version 5, General Circulation Model, *J. Atmos. Sci.*, *66*, 627–646.

Palmer, P. I., et al. (2003), Inverting for emissions of carbon monoxide from Asia using aircraft observations over the western Pacific, *J. Geophys. Res.*, *108*(D21), 8828.

Park, M., W. J. Randel, A. Gettleman, S. T. Massie, and J. H. Jiang (2007), Transport above the Asian summer monsoon anticyclone inferred from Aura MLS tracers, *J. Geophys. Res. 112*, D16309.

Park, M., W. J. Randel, L. K. Emmons, and N. J. Livesey (2009), Transport pathways of carbon monoxide in the Asian summer monsoon diagnosed from Model of Ozone and Related Tracers (MOZART), *J. Geophys. Res.*, *114*, D08303.

Parrington, M., et al. (2008), Estimating the summertime tropospheric ozone distribution over North America through assimilation of observations from the Tropospheric Emission Spectrometer, *J. Geophys. Res.*, *113*, D18307.

Parrington, M., et al. (2012), The influence of boreal biomass burning emissions on the distribution of tropospheric ozone over North America and the North Atlantic during 2010, *Atmos. Chem. Phys.*, *12*, 2077–2098.

Pétron, G., et al. (2002), Inverse modeling of carbon monoxide surface emissions using Climate Monitoring and Diagnostics Laboratory network observations, *J. Geophys. Res.*, *107*(D24), 4761.

Pétron, G., et al. (2004), Monthly CO surface sources inventory based on the 2000– 2001 MOPITT satellite data, *Geophys. Res. Lett.*, *31*, L21107.

Scharffe, D., F. Slemr, C. A. M. Brenninkmejer, and A. Zahn (2012), Carbon monoxide measurements onboard the CARIBIC passenger aircraft using UV resonance fluorescence, *Atmos. Meas. Tech. Discuss.*, *5*, 2681–2702

Singh, K., et al. (2011), Construction of non-diagonal background error covariance matrices for global chemical data assimilation, *Geosci. Model Dev.*, *4*, 299–316

Tost, H., et al. (2010), Uncertainties in atmospheric chemistry modelling due to convection parameterisations and subsequent scavenging, *Atmos. Chem. Phys.*, *10*, 1931.

van der Werf, G. R., et al. 2006, Interannual variability in global biomass burning emissions from 1997 to 2004, *Atmos. Chem. Phys.*, *6*, 3423–3441.

Vestreng, V., and H. Klein, (2002), Emission data reported to UNECE/EMEP. Quality assurance and trend analysis and Presentation of WebDab, Norwegian Meteorological Institute, Oslo, Norway, MSC-W Status Report.

Worden, H. M., et al. (2010), Observations of near-surface carbon monoxide from space using MOPITT multispectral retrievals, *J. Geophys. Res.*, *115*, D18314.

Zhang, Q., et al. (2009), Asian emissions in 2006 for the NASA INTEX-B mission, *Atmos. Chem. Phys.*, *9*, 5131–5153.